specific rate for reduction of the indicated branched hydroxylamine were comparable to that found here for $(CH_3)_2NHOH^+$.

Although a portion of the second organic product, $C_6H_5CH(CH_3)OH$, doubtless arises from hydrolysis of the oxime and reduction of the resulting ketone, we cannot exclude the possibility that some of this alcohol results from an alternative reductive sequence beginning with attack at the N–O bond (7). If this route is significant, the close adherence to mon-

$$Co^{I}: + HO(H)N^{+}=C< \rightarrow Co^{III}OH + NH=C< \quad (7)$$

$$>C=NH \xrightarrow{H_3O^+} >C=O \xrightarrow[H^+]{Co^I} >CHOH \quad (8)$$

omial kinetics again requires that the initial step (7) be slower than succeeding steps. In particular, the specific rate for reduction of acetophenone to the alcohol must exceed that for reduction of the oxime to the rapidly hydrolyzed imine. Although the latter condition appears to be in accord with experiment,[34] additional work is needed to evaluate the extent to which this path contributes.

Acknowledgment. The authors are indebted to Professor Harry B. Mark, Jr., for helpful discussions.

Registry No. NH_4^+, 14798-03-9; $C_6H_5CH(CH_3)NH_2$, 98-84-0; $C_6H_5CH(CH_3)OH$, 98-85-1; NO_3^-, 14797-55-8; $(CH_3)_2C=NOH$, 127-06-0; $C_6H_5COCH_3$, 98-86-2; $NH_2OH\cdot HClO_4$, 15588-62-2; $CH_3NHOH\cdot HClO_4$, 88905-37-7; $CH_3ONH_2\cdot HClO_4$, 28219-79-6; $(CH_3)_2NOH\cdot HClO_4$, 88905-38-8; $(C_2H_5)_2NOH\cdot HClO_4$, 88905-39-9; NH_2OSO_3H, 2950-43-8; $C_6H_5C(=NOH)CH_3$, 613-91-2; $HON(SO_3)_2^{2-}\cdot 2K^+$, 21049-67-2; $CH_3NHOCH_3\cdot HClO_4$, 88905-40-2; $HONHSO_3^-\cdot K^+$, 13768-26-8; hydroxocobalamin hydrochloride, 15041-07-3; cob(I)alamin, 18534-66-2.

(34) Preliminary experiments by P.N.B. indicate that acetophenone is reduced by cob(I)alamin at a specific rate near 12 M^{-1} s^{-1} in 0.088 M $HClO_4$ at 25 °C. The observed rate constant for reduction of the oxime at this acidity is 6.2 M^{-1} s^{-1}, of which a maximum of 77%, or 4.8 M^{-1} s^{-1}, pertains to the alcohol-generating path.

Contribution from the Energy Systems Group, Rockwell International Corporation, Canoga Park, California 91304

Electrochemical Studies of Graphite Oxidation in Sodium Carbonate Melt

GARY B. DUNKS

Received June 20, 1983

The oxidation of spectroscopic grade graphite in sparged beds of sodium carbonate employing air, nitrogen, and carbon dioxide was investigated at 900 °C by using electrochemical techniques. Evidence for the formation of metallic sodium suggested that a first step in the oxidation process was the reduction of sodium ion by graphite. The positive centers thus generated in the graphite matrix apparently reacted with oxyanions in the melt to produce carbon monoxide. The oxidation rate of a graphite electrode using carbon dioxide containing sparge gas was increased by application of positive potentials and decreased by application of negative potentials, which supports such an ionic mechanism. The initial rates of graphite oxidation using nitrogen or carbon dioxide sparge were approximately equal and were 6.5 times slower than the rate using air. Sequences of reactions are proposed for the oxidation of graphite using air, carbon dioxide, and nitrogen sparge gases in sodium carbonate melt.

Introduction

Alkali-metal carbonates are effective catalysts for the gasification of carbonaceous materials including coal. The mechanisms through which these gasification processes proceed however are not well understood.[1] In previous studies directed toward the elucidation of the mechanism of graphite oxidation in sparged beds of molten sodium carbonate, oxidation rates were determined as functions of oxygen and carbon dioxide concentrations of the sparge gas, melt temperature, sulfate concentration, graphite loading, and graphite surface area.[2-4] Subsequently, electrochemical measurements showed that oxide, peroxide, and superoxide ions and possibly the complex ions peroxycarbonate and peroxydicarbonate exist in molten sodium carbonate and how the concentrations of the melt species changed with perturbations of the oxygen and carbon dioxide concentrations of the sparge gas.[5]

The results of work in which the relative concentrations of melt species were monitored electrochemically during graphite oxidation in molten sodium carbonate using air, carbon dioxide, and nitrogen sparge gases are reported here.

Experimental Section

Materials. Air ("breathing air": 20.9% oxygen, 0.03% carbon dioxide, and 78.1% nitrogen), oxygen (99.993%), carbon dioxide (99.99%), nitrogen (99.999%), and calibration gas mixtures were obtained from and analyzed by Airco.

Sodium carbonate (Baker anhydrous reagent grade, 99.5%) contained nitrogen compounds (N, 0.001%), phosphorus (PO_4, 0.01%), silica (SiO_2, 0.005%), sulfur (SO_4, 0.003%), and iron (Fe, 5 ppm).

The graphite was spectroscopic grade SP2-Z powder (>80% graphitic) prepared from petroleum coke with use of a proprietary binder and heat treated at 3000 °C (Union Carbide Corp.). The total ash content was <2 ppm; impurities present were iron (0.3 ppm), magnesium (0.2 ppm), and silicon (0.4 ppm). Prior to use, the graphite was sieved with 80-mesh (0.0180-cm) and 100-mesh (0.0150-cm) screens. All of the experiments were performed with the −80 to +100 mesh fraction, which had a specific surface area of 1.01 m^2/g (BET, nitrogen, or krypton adsorption measured by Micromeritics Instrument Corp., Norcross, GA 30071). Graphite electrodes (0.32 × 30.5 cm cylinders) were ACKSP spectroscopic grade containing <6 ppm impurities and <1 ppm ash (Union Carbide Corp.). The graphite electrodes were lowered into the cell and suspended on platinum lead wires.

Apparatus. The apparatus (described in detail previously[5]) consisted of an electrochemical cell contained in a tube furnace. A three-electrode system was used in which the working electrode consisted of a rectangular gold sheet (1 × 0.5 × 0.025 cm) spot welded to 0.05-cm (diameter) gold lead wire and allowed to extend 1 cm into the melt providing an effective geometric surface area of 1.16 cm^2. The counterelectrode was a gold-foil cylinder (4 × 7 cm) that rested on the bottom of the crucible and was connected by a 0.05-cm (diameter) gold lead wire. The reference electrode consisted of a 0.05-cm (diameter) gold wire that dipped into the melt within an alumina tube that rested on the bottom of the crucible. The melt within the tube was in contact with a slow stream (40 mL/min) of oxygen (33%) and carbon dioxide (67%). This reference electrode has been described in detail.[6] All parts of the apparatus contacting the molten sodium

(1) KcKee, D. W. *Chem. Phys. Carbon* **1981**, *16*, 1.
(2) Stelman, D.; Darnell, A. J.; Christie, J. R.; Yosim, S. J. *Proc. Int. Symp. Molten Salts* **1976**, 299.
(3) Dunks, G. B.; Stelman, D.; Yosim, S. J. *Carbon* **1980**, *18*, 365.
(4) Dunks, G. B.; Stelman, D.; Yosim, S. J. *Inorg. Chem.* **1982**, *21*, 108.
(5) Dunks, G. B.; Stelman, D. *Inorg. Chem.* **1983**, *22*, 2168.

0020-1669/84/1323-0828$01.50/0

carbonate were constructed of fine gold or 99.8% alumina (Coors AD-998).

Sparge gas mixtures (oxygen, carbon dioxide, and nitrogen) were prepared with a gas blender (Medicor, Inc., Model PGM-3) that was modified to accept commands from an HP-9825B computer through an HP-98032A, 16-bit interface.[7] Thus, a preprogrammed sequence of sparge gas compositions could be prepared as a function of time. The sparge gas was passed through the melt at 0.239 L/min (25 °C (1 atm)) by using a peristaltic pump (Masterflex, Cole-Parmer Inc.) equipped with Tygon tube. Part of the exhaust gas from the cell was pumped through an oxygen analyzer (Beckman Model 755) and carbon dioxide and carbon monoxide analyzers (Horiba Model PIR-2000). Data from the analyzers, together with melt and furnace temperatures and time, were gathered each 30 s, partially reduced, and stored on magnetic tape by using a data acquisition system. These data could be recalled and plotted with use of an HP-9872A plotter. Electrochemical measurements were made with a Princeton Applied Research Model 170 system. Curve fitting was accomplished with an HP-9845B computer.

A Pyrex solids addition device fitted with a straight-bore Teflon stopcock could be installed at the top of the sparge tube. The sparge gas flowed through a tee below the stopcock and then down the sparge tube. A weighed sample of the solid to be added to the melt was placed in a sealed chamber above the stopcock. Turning the stopcock allowed the solid to drop directly down the sparge tube with the sparge gas into the melt.

Procedure. The internals of the electrochemical cell (crucible, heat shields, counterelectrode, etc.) were assembled and attached to the cover plate. The remaining electrodes, thermowell, and sparge tube were fitted through the cover plate and sealed. The crucible was charged with 175 g of sodium carbonate (~90 mL of melt) and the assembly slowly lowered (over ~6 h) into the containment vessel that was maintained at 900 ± 2 °C. When the crucible was in final position, the cover plate was secured to the containment vessel collar with bolts. The working electrode, reference electrode, and sparge tube were lowered into the melt, which was then sparged with carbon dioxide for an overnight period to convert the "oxides" present to carbonate. During this time, the reference electrode gas was allowed to "equilibrate" with the reference melt.

The majority of the electrochemical measurements were controlled-potential sweeps (0.5 V/s) from the rest potential (cathodically to −1.40 V and anodically to +0.10 V). Prior to the cathodic sweep, the pumps that supplied the sparge gas and extracted the analytical sample gas (exhaust) were stopped for approximately 15 s. The sweep was made, and the pumps were started and allowed to run 15 s. The pumps were again stopped for 15 s, and the anodic sweep was initiated at the rest potential. After the anodic sweep, the pumps were started and allowed to run until the next electrochemical measurement. In air-sparged sodium carbonate, evidence for the existence of at least eight overlapping electrochemical waves (five cathodic and three anodic including the cutoff waves) was observed. Because of the complexity of the observed current–potential curves, analysis by simple peak-current and peak-potential measurements was found to be inadequate. Instead, composite curves made up of the algebraic sum of eight computer-generated theoretical waves using current and potential functions for charge transfers at stationary electrodes developed by Nicholson and Shain[8] were fitted to the experimental curves using a nonlinear least-squares procedure.[5]

Results

Current–Potential Curves of Air-Sparged Sodium Carbonate. Cyclic triangular-sweep and single-sweep scans of molten sodium carbonate (900 °C) after air sparge for 48 are shown in Figure 1. The cyclic scan (Figure 1a) shows that the initial cathodic wave is reversible (cathodic peak potential, $E_{p,c}$ = −0.56 V; anodic peak potential, $E_{p,a}$ = −0.37 V) with n = 1.17. The second cathodic wave ($E_{p,c}$ = −1.06 V) is irreversible as shown by the cyclic scan and by an observed cathodic shift

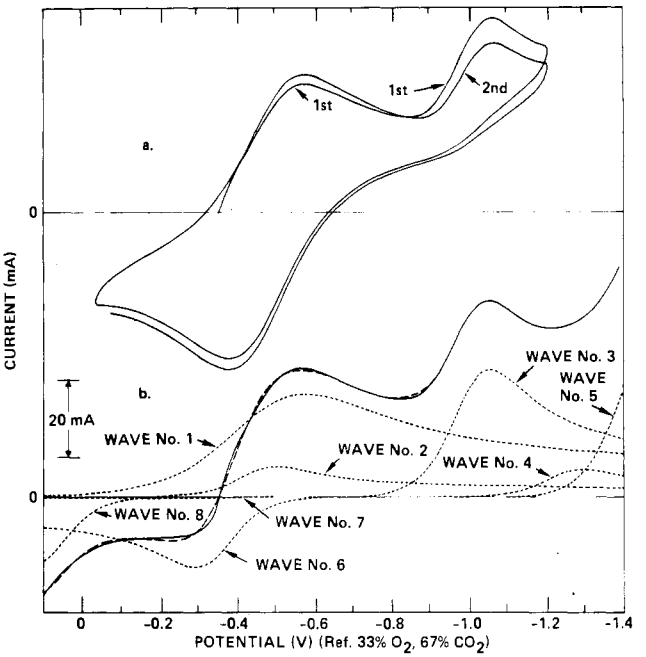

Figure 1. Current–potential curves of sodium carbonate (900 °C) after air sparge: (a) cyclic scan beginning cathodic from the rest potential; (b) single-sweep scans both cathodic and anodic from the rest potential (solid line) with the computer-generated composite curve (dashed line) and component waves indicated (dotted lines).

Table I. Proposed Assignments of Waves Observed in Sodium Carbonate, 900 °C, Air Sparge[5]

wave	E_p,[a] V	eq	
1	−0.56	$O_2^- + e^- \rightarrow O_2^{2-}$	(1)
2	−0.49	$CO_4^{2-} + 2e^- \rightarrow CO_3^{2-} + O^{2-}$	(2)
3	−1.06	$C_2O_6^{2-} + 2e^- \rightarrow 2CO_3^{2-}$	(3)
4	−1.20	?	
5	<−1.40	$2CO_2 + 2e^- \rightarrow CO + CO_3^{2-}$	(4)[9]
6	−0.40	$CO_3^{2-} + O^{2-} \rightarrow 2e^- + CO_4^{2-}$	(5)
7	−0.31	$O_2^{2-} \rightarrow e^- + O_2^-$	(6)
8	>0.10	$CO_3^{2-} \rightarrow 2e^- + {}^1/_2O_2 + CO_2$	(7)[10]

[a] Reference: 33% O_2, 67% CO_2, Au.

with increased sweep rate as predicted by theory.[8] The results of the curve-fitting procedure applied to the single-sweep scan (Figure 1b) show that the root-mean-square difference between the experimental curve (solid line) and the computer-synthesized composite curve (dashed line) is 0.567 mA over the 1.5-V range. The eight component waves of the composite curve are shown (dotted lines). The analysis shows that the cathodic part of the single-sweep scan of sodium carbonate melt under air sparge is composed largely of a 1-electron wave (wave 1) and a 2-electron wave (wave 3) with smaller contributions from the 2-electron waves (waves 2 and 4) (excluding the 2-electron cutoff wave, wave 5). The anodic part of the scan is composed of a 2-electron wave (wave 6) with a very small contribution from a 1-electron wave (wave 7) (excluding the 2-electron cutoff wave, wave 8). Assignments of the waves and the rationale for those assignments were reported previously and are presented in Table I.[5]

Graphite Oxidation (Air Sparge). After treatment with carbon dioxide, the melt was sparged with air for 48 h to achieve approximate steady state. Without interrruption of the air sparge, 0.2292 g (0.019 mol) of graphite was charged to the melt, which marked t = 0. During the course of the 600-min experiment, the compositions of the exhaust gas and melt were monitored. The exhaust gas oxygen (open circles) and carbon dioxide (open triangles) concentrations are presented in Figure 2. The integrals of the curves indicated that

(6) Borucka, A. *Adv. Chem. Ser.* **1969**, *No. 90*, 242.
(7) Modification was made by Dr. C. A. Cutler, Medicor Inc.
(8) Nicholson, R. S.; Shain, I. *Anal. Chem.* **1964**, *36*, 706.
(9) Lorenz, P. K.; Janz, G. J. *J. Electrochem. Soc.* **1971**, *118*, 1550.
(10) Bartlett, H. E.; Johnson, K. E. *J. Electrochem. Soc.* **1967**, *114*, 457.

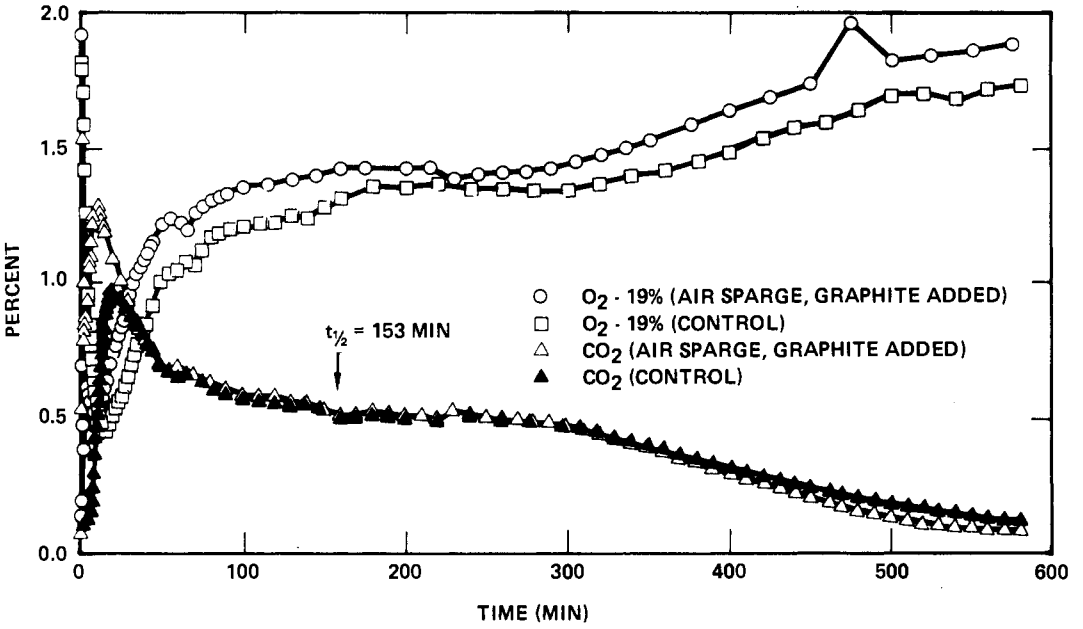

Figure 2. Exhaust gas oxygen (~19.00%) and carbon dioxide concentrations measured during air-sparged graphite oxidation and control experiments plotted as a function of reaction time.

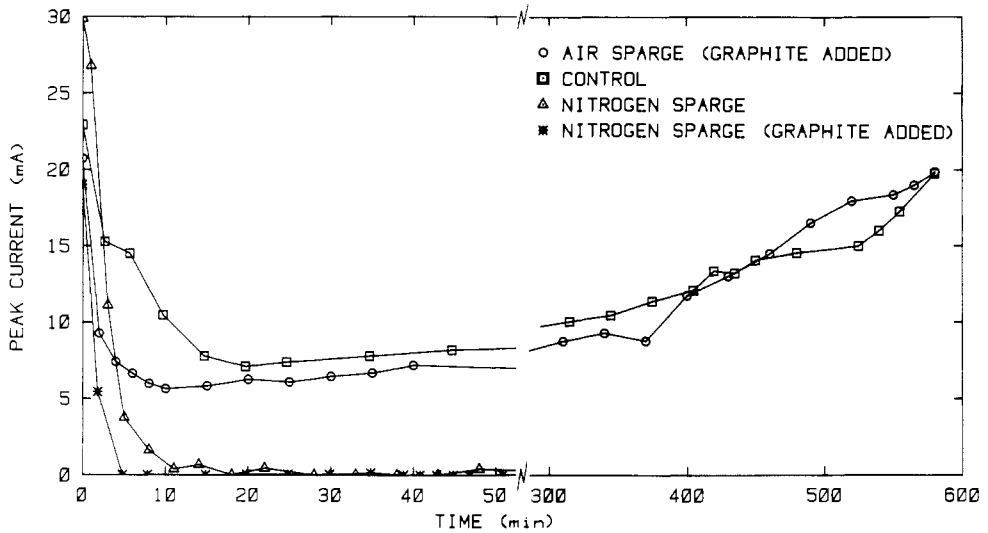

Figure 3. Peak currents of the superoxide ion wave (wave 1) measured during graphite oxidation, the control experiment, nitrogen sparge, and nitrogen sparge with added graphite plotted as a function of reaction time.

0.025 of mol of oxygen was consumed and 0.019 mol of carbon dioxide was evolved. These values are very close to the quantity of graphite charged, which confirms the previous finding that the only product of graphite oxidation evolved under these conditions is carbon dioxide.[2-4] Thus, the instantaneous carbon dioxide concentration of the exhaust gas is an accurate measure of the rate of the oxidation process. The time at which half of the graphite had been consumed ($t_{1/2}$) was 153 min. Inspection of Figure 2 shows that the exhaust gas carbon dioxide concentration curve consisted of three regions. In the first region, lasting for approximately the first 100 min of the experiment, the oxidation rate increased rapidly, maximized, and then decreased rapidly. This was probably due to the rapid reaction of graphite with the relatively high concentration of oxidant species initially present in the air-sparged melt. In the second region, from approximately 100 to about 300 min, the oxidation rate was relatively constant. In this region, the rate is approximately half-order with respect to both oxygen pressure and graphite surface area[4] and is therefore affected by both parameters. In the third region, from approximately 300 min until the graphite was consumed, the oxidation rate gradually decreased. The rate in the third region remains half-order in oxygen; however, the graphite surface area dependence increases to 0.78.[4] This suggests that the rate is primarily limited by the available graphite surface area near the end of the experiment.

The peak currents of the electrochemical waves observed as a function of time during the experiment are shown in Figures 3-8. Excluding the cathodic cutoff wave (wave 5), the anodic cutoff wave (wave 8), and the peroxide ion wave (wave 7), which changed little, all of the waves decreased rapidly after the addition of graphite. This suggests that the species whose peak currents (i.e., concentrations) exhibited significant change may have reacted with the graphite. However, the only gaseous product of graphite oxidation evolved under these conditions is carbon dioxide,[2-4] and all of the electroactive species that exhibited significant change in this experiment possess strong negative dependences on carbon dioxide pressure.[5]

Control Experiment. To separate the effects of the graphite added to the melt and carbon dioxide produced by oxidation of the graphite on the electroactive melt species, a control

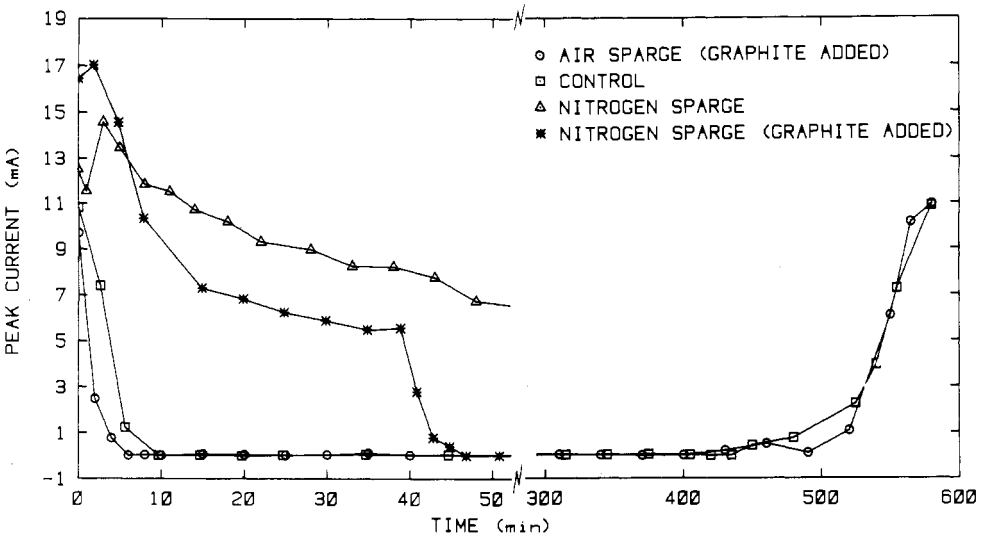

Figure 4. Peak currents of the peroxycarbonate ion wave (wave 2) measured during graphite oxidation, the control experiment, and nitrogen sparge plotted as a function of reaction time.

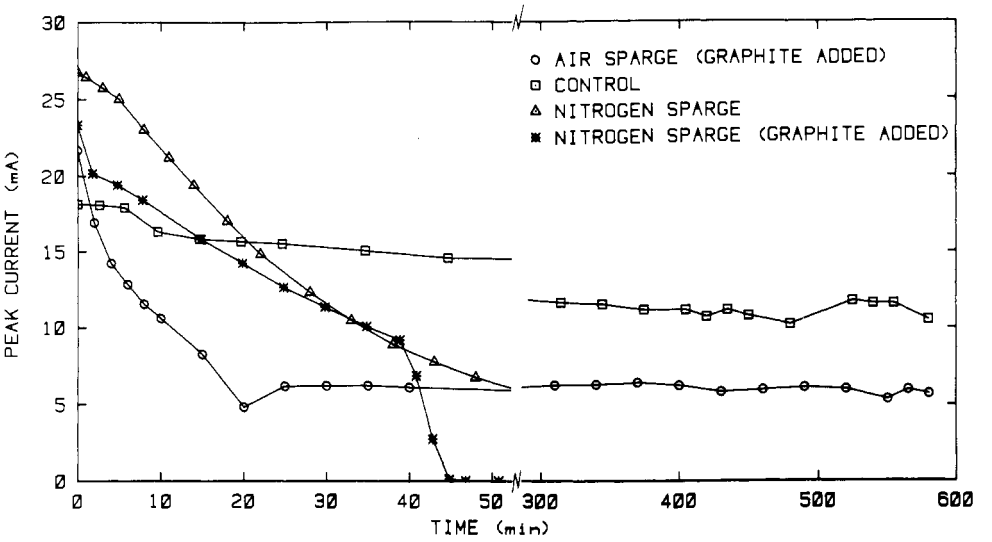

Figure 5. Peak currents of the peroxydicarbonate ion wave (wave 3) measured during graphite oxidation, the control experiment, and nitrogen sparge plotted as a function of reaction time.

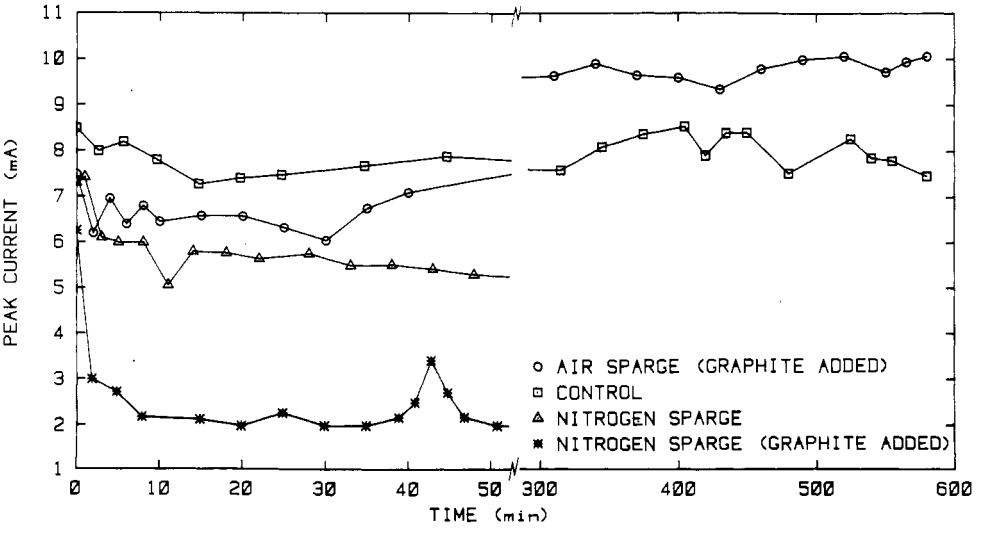

Figure 6. Peak currents of wave 4 measured during graphite oxidation, the control experiment, and nitrogen sparge plotted as a function of reaction time.

experiment was conducted in which the melt was prepared with carbon dioxide and air as described above then sparged with gas whose composition as a function of time was identical with the exhaust gas composition of the graphite oxidation experiment above. That is, in a separate experiment, the exhaust gas data from the graphite oxidation experiment were fed by

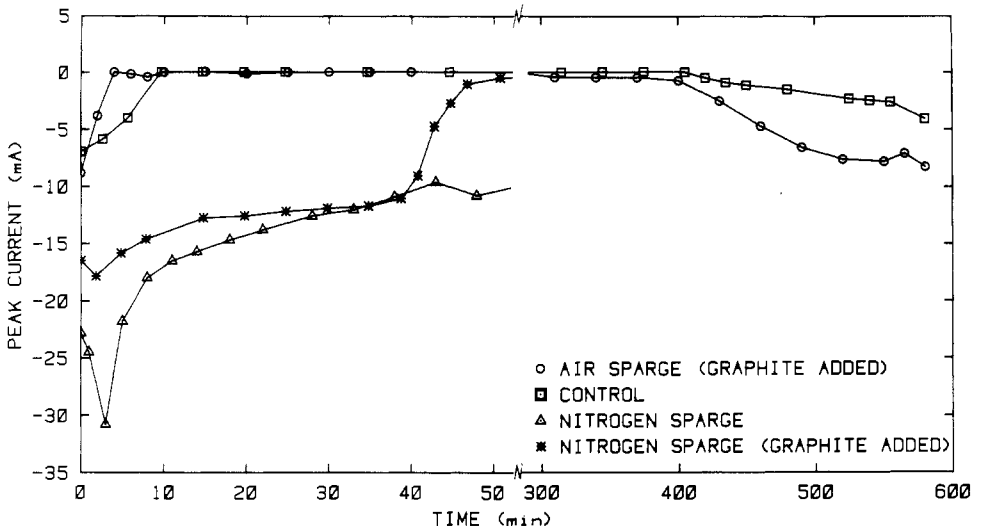

Figure 7. Peak currents of the oxide ion wave (wave 6) measured during graphite oxidation, the control experiment, and nitrogen sparge plotted as a function of reaction time.

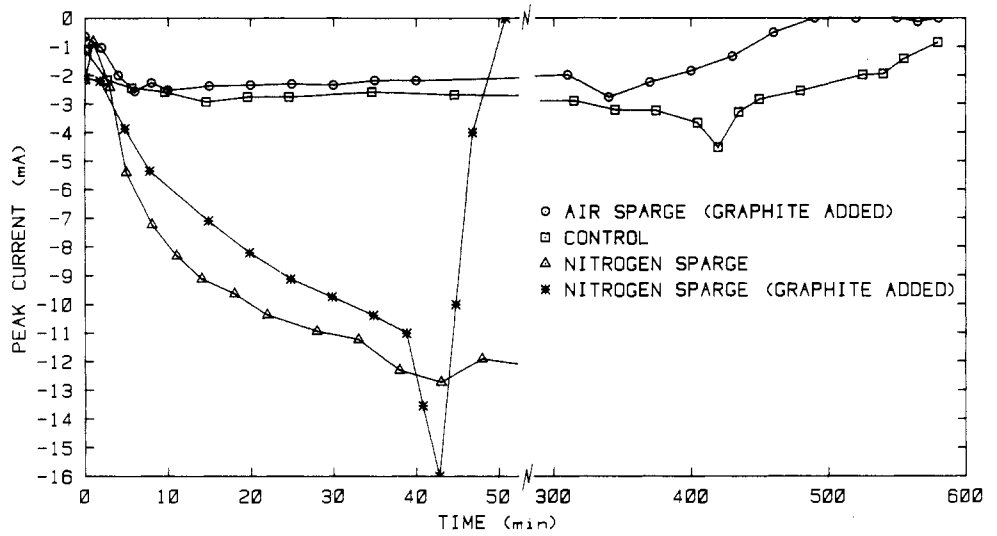

Figure 8. Peak currents of the peroxide ion wave (wave 7) measured during graphite oxidation, the control experiment, and nitrogen sparge plotted as a function of reaction time.

the computer to the gas blender so that the sparge gas composition simulated the conditions that existed during the graphite oxidation experiment. Thus, with the exception that no graphite was present in the control experiment, the conditions that existed in the melt were very nearly identical in both the graphite oxidation experiment and the control experiment. The exhaust gas and melt compositions were monitored as described above. The exhaust gas oxygen (open squares) and carbon dioxide (filled triangles) concentrations of the control experiment are presented in Figure 2. Except for the first 30 min of the control experiment, where carbon dioxide was being absorbed by the melt, the exhaust gas carbon dioxide concentrations in both the graphite oxidation and control experiments were nearly identical, while the exhaust gas oxygen concentration of the control experiment was approximately 0.15% less than that of the oxidation experiment.

The peak current measurements (Figures 3–8) after the addition of graphite to the air-sparged melt, when compared to those of the control experiment, showed that peak currents of superoxide (wave 1), peroxycarbonate (wave 2), peroxide (wave 7), and oxide (wave 6) ions behaved in the same way whether or not graphite was present in the melt. Of the observable electroactive species, only the peroxydicarbonate ion (wave 3) exhibited a significant peak current difference in the two experiments, which suggests that the peroxydicarbonate ion reacted directly with graphite, while the peak currents of the remaining melt species in both experiments were primarily a reflection of the sparge gas composition.

Nitrogen Sparge Experiments. Melts that had been prepared with carbon dioxide and air as described above were sparged with nitrogen in two separate experiments.

In the first experiment, the nitrogen sparge was allowed to proceed for 176 min to provide a base line for the second experiment. The carbon dioxide concentration of the exhaust gas, which was equilibrated at approximately 0.03% during the air sparge, increased slightly to approximately 0.05% when the nitrogen sparge was begun and then decreased again. The oxygen concentration of the exhaust gas decreased rapidly from 20.9% to ~0.10% over the first 40 min of the nitrogen sparge and then continued to decrease more slowly. The peak currents of all of the waves (with the exception of wave 7, peroxide ion) decreased during the nitrogen sparge. After 40 min, the peak currents of all of the waves (except for wave 1, superoxide ion, which had decreased to near zero) remained significant (Figures 3–8). Thus, the effect of graphite added to the melt on the anions that had measurable concentrations at that point could be determined.

In the second experiment, the nitrogen sparge was allowed to proceed for 40 min and then 0.2297 g (0.019 mol) of graphite was added without interruption of the nitrogen flow. The

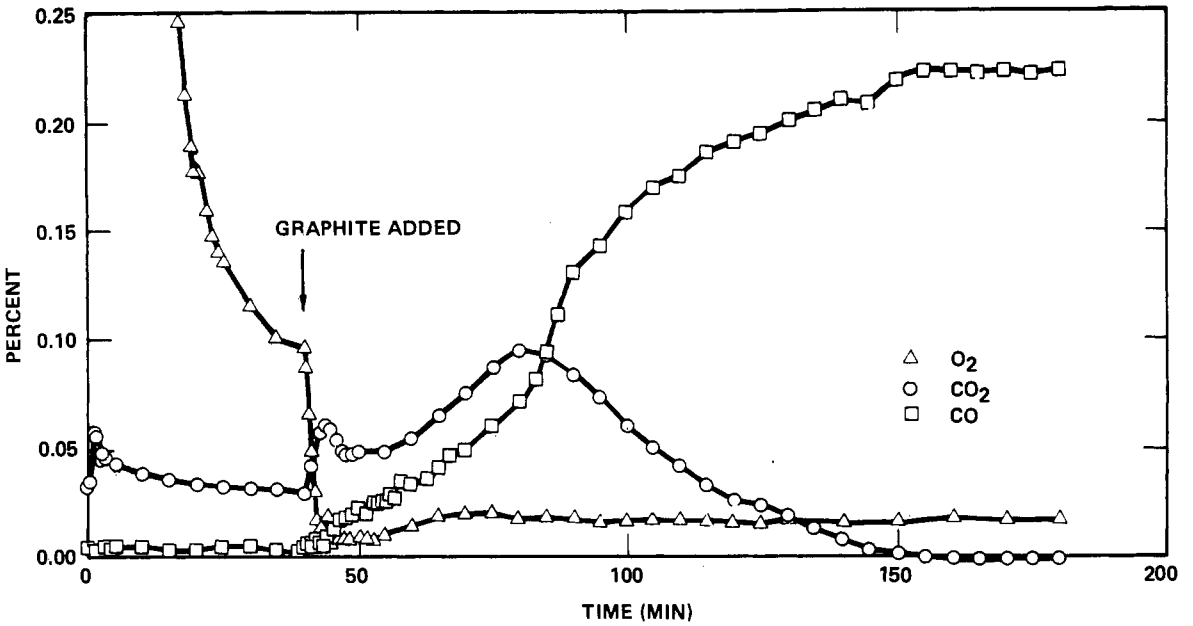

Figure 9. Exhaust gas oxygen, carbon dioxide, and carbon monoxide concentrations of nitrogen-sparged melt to which graphite was added.

exhaust gas oxygen, carbon dioxide, and carbon monoxide concentration vs. time curves are shown in Figure 9, and peak currents vs. time are shown in Figures 3–8. The oxygen concentration of the exhaust gas decreased to near zero immediately after the addition of graphite and remained very low throughout the remainder of the experiment. For 40 min after the addition of graphite, the exhaust gas concentrations of both carbon dioxide and carbon monoxide increased at approximately the same rate. The carbon dioxide concentration then maximized at ~0.10% and decreased over the next 80 min to near zero. The carbon monoxide concentration continued to increase over the next 80 min to a relatively constant concentration of 0.23%. Addition of graphite caused an immediate cathodic shift of the rest potential from −0.553 to −1.115 V, which continued to shift more slowly to a final value of −1.370 V. The shift of the rest potential was accompanied by decreases in the peak currents of all of the waves except waves 4 (unidentified) and 7 (peroxide ion), which increased initially and then also decreased. Approximately 5 min after the addition of graphite, an anodic wave at about −0.92 V appeared that gave way after 10 min to a larger anodic wave at about −0.56 V (Figure 10). These two anodic waves have been observed previously in carbonate melt sparged with carbon monoxide/carbon dioxide mixtures and were assigned to the oxidation of carbon monoxide and the proposed CO_2^{2-} ion, respectively.[11] The mechanism proposed[11] for the formation of CO_2^{2-} ion is represented by eq 8 and 9, and the

$$Na_2CO_3 \rightleftarrows Na_2O + CO_2 \quad (8)$$

$$Na_2O + CO \rightleftharpoons Na_2CO_2 \quad (9)$$

oxidation of the CO_2^{2-} ion is represented by eq 10. The

$$CO_2^{2-} \rightarrow 2e^- + CO_2 \quad (10)$$

proposed mechanism of the oxidation of carbon monoxide is represented by eq 11–13. The rest potential observed in these

$$CO \rightarrow e^- + CO^+ \quad (11)$$

$$CO^+ + CO_3^{2-} \rightarrow CO_2^- + CO_2 \quad (12)$$

$$CO_2^- \rightarrow e^- + CO_2 \quad (13)$$

(11) Borucka, A.; Appleby, A. J. *J. Chem. Soc., Faraday Trans.* **1977**, *73*, 1420.

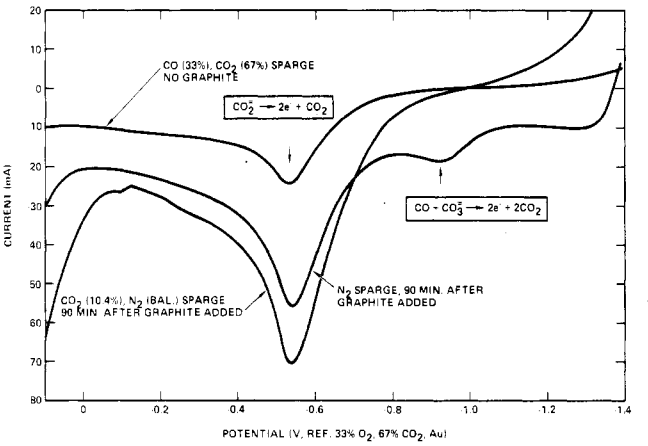

Figure 10. Current–potential curves of sodium carbonate (900 °C) indicating the presence of carbon monoxide and the CO_2^{2-} ion.

studies was approximately −0.92 V, which suggests that the potential was defined by the oxidation of carbon monoxide.[11] Indeed, the potential of the standard carbon monoxide/carbon dioxide reference electrode relative to the potential of the standard oxygen/carbon dioxide reference electrode at 900 °C is −0.934 V.[6] The fact that the rest potential observed in the present work immediately shifted cathodically to −1.115 V within 5 min after the addition of graphite and ultimately equilibrated at about −1.370 V suggests the presence of a more easily oxidized species, possibly sodium metal.

The peak current of the superoxide ion wave (wave 1) in the nitrogen-sparged experiment shown in Figure 3 decreased at approximately the same rate as it did in the air-sparged graphite oxidation experiment, which suggests that the concentration of superoxide ion responded primarily to a decrease in the activity of oxygen in the melt (eq 14), not to the direct

$$2NaO_2 \rightleftarrows Na_2O_2 + O_2 \quad (14)$$

reaction with graphite. This is supported by the fact that the peak current decreased to near zero in the absence of oxygen (i.e., nitrogen sparge). No change was observed after the addition of graphite under nitrogen sparge. The peak current of the peroxycarbonate ion wave (wave 2) in the nitrogen-sparged experiment shown in Figure 4 initially increased and then decreased slowly over the next 176 min. Thus, removal of oxygen from the system (i.e., nitrogen sparge) had much

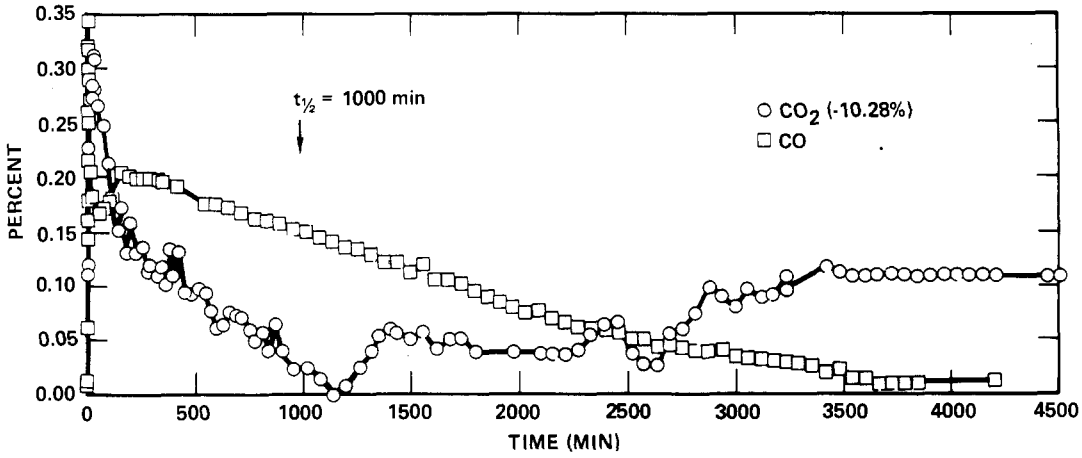

Figure 11. Exhaust gas carbon dioxide (−10.28%) and carbon monoxide concentrations of graphite oxidation using carbon dioxide (10.40%)/nitrogen (balance) sparge gas.

less effect on the concentration of the peroxycarbonate ion than the addition of graphite and/or the carbon dioxide produced by the air-sparged oxidation of the graphite.

Graphite Oxidation (Carbon Dioxide Sparge). Melt was sparged with a mixture of carbon dioxide (10.40%) and nitrogen (balance) overnight and then 0.2306 g (0.019 mol) of graphite was added without interruption of the sparge gas flow. Under such conditions, only the cutoff waves (waves 5 and 8) were observed, and therefore, the melt was essentially pure sodium carbonate. Carbon dioxide and carbon monoxide were produced immediately (Figure 11). The exhaust gas concentration of carbon monoxide increased from 0 to 0.34% in the first 11 min and then decreased rapidly to a relatively constant value of ~0.20%. This concentration of carbon monoxide (0.20%) was virtually identical with that observed when graphite was added to nitrogen-sparged melt (0.23%, Figure 9), which suggests that the rate of oxidation was not dependent on the sparge gas (i.e., the rate-determining step is the same under carbon dioxide or nitrogen-sparged conditions). After ~300 min, the concentration of carbon monoxide began to decrease slowly to zero after 3660 min. The integral of the exhaust gas carbon monoxide concentration vs. reaction time curve represented 0.035 mol or about 92% of the quantity expected based upon eq 15. The time required to consume

$$C + CO_2 \rightleftarrows 2CO \qquad (15)$$

half of the graphite ($t_{1/2}$ = 1000 min) was approximately 6.5 times that required in the air-sparged graphite oxidation experiment above. The exhaust gas concentration of carbon dioxide increased from the initial concentration of 10.40% to 10.60% over the first 24 min and then decreased slowly to approximately 10.33% after 800 minutes. The concentration remained nearly constant until approximately 2600 min had elapsed and then slowly increased back to the sparge gas concentration (10.40%) after 3660 min. The integral of the exhaust gas carbon dioxide concentration vs. reaction time curve indicated that approximately 1.7 mmol was initially produced (over the first 250 min) and then 0.019 mol was consumed during the remainder of the experiment. The rest potential of the system moved cathodically from −0.315 to −0.925 V in the first 7 min after the addition of graphite, and the anodic wave at approximately −0.54 V assigned to CO_2^{2-} ion began to appear. The peak current of the wave increased from 0 to −69.03 mA over the first 300 min, remained relatively constant until approximately 2000 min had elapsed, and then began to decrease (Figure 12).

Sodium Metal Addition. The cathodic shift of the rest potential to −1.370 V after the addition of graphite to nitrogen-sparged melt suggested the possible presence of metallic sodium. To determine the effect of sodium, the melt was

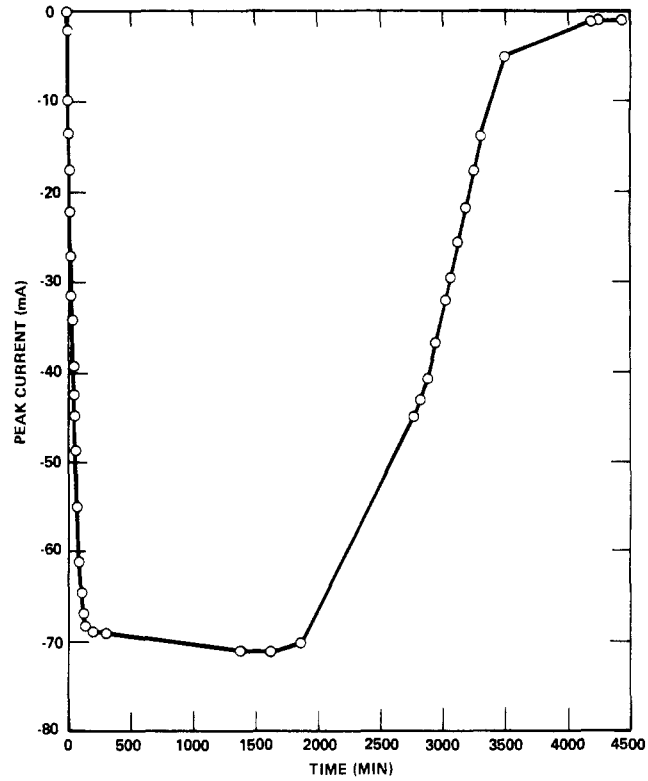

Figure 12. Peak current of the CO_2^{2-} ion wave measured during graphite oxidation using carbon dioxide (10.40%)/nitrogen (balance) sparge gas.

sparged with carbon dioxide overnight and then sparged with nitrogen for 100 min prior to the addition of sodium metal (0.0237 g, 1.03 mmol). This procedure first converted "oxides" to carbonate and then purged the system of excess carbon dioxide without significant decomposition of the melt. The immediate effect of the sodium was a cathodic shift of the rest potential from −0.561 to −1.188 V. After ~2 min, an anodic wave appeared at −0.86 V (carbon monoxide), which slowly decreased from the initial peak current of −15.80 to −4.80 mA after 400 min. Exhaust gas analysis showed that carbon monoxide (trace) was evolved during only the first 6 min after the addition of sodium. The exhaust gas carbon dioxide concentraiton decreased slightly with the addition of sodium (from 0.09% to 0.05%) and remained relatively constant over the course of the experiment. After 400 min, the nitrogen sparge gas was stopped and the melt was sparged with a mixture of carbon dioxide (10.40%) and nitrogen (balance). The rest potential shifted from −1.18 to −0.933 V immediately

and then continued to move anodically more slowly to −0.285 V after 17 h. The peak current of the anodic wave at −0.86 V decreased rapidly when the carbon dioxide sparge was initiated.

After the melt had been sparged with a mixture of carbon dioxide (10.40%) and nitrogen (balance) for 24 h, a second sample of sodium metal (0.0233 g, 1.01 mmol) was added. The rest potential shifted from −0.285 to −0.934 V within the first minute and then slowly moved positive to −0.761 V after 160 min. After 160 min had elapsed, the rest potential moved rapidly to −0.325 V. The integrals of the exhaust gas carbon dioxide and carbon monoxide concentration vs. time curves indicated that 0.351 mmol of carbon dioxide was consumed over the first 50 min and that 0.572 mmol of carbon monoxide was produced. Although most of the carbon monoxide was produced during the first 50 min, evolution continued until 160 min had elapsed. The sudden positive shift of the rest potential after 160 min corresponded to the cessation of carbon monoxide evolution. An anodic wave at −0.56 V (CO_2^{2-} ion) appeared in the first minute after sodium addition. The peak current increased to −11 mA, remained constant for about 40 min, and then began to decrease to near zero after 120 min.

These results indicate that sodium metal reacted with carbon dioxide to produce carbon monoxide. Under nitrogen-sparged conditions, where the concentration of carbon dioxide was low, the only wave observed was that assigned to the oxidation of carbon monoxide, and the negative shift of the rest potential to ~−1.19 V suggests the presence of metallic sodium in the system. With relatively high carbon dioxide concentration, the predominant wave was that assigned to the oxidation of the CO_2^{2-} ion (−0.56 V), and the shift of the rest potential to only −0.934 V suggests that the concentration of sodium metal was significantly lower than in the nitrogen-sparged experiment above. A sequence of reactions consistent with the data is represented by eq 8, 9, and 16 with the overall process represented by eq 17. The carbon dioxide consumed (0.351 mmol) and carbon monoxide evolved (0.572 mmol) after sodium was added to melt sparged with carbon dioxide (10.40%)/nitrogen suggest that carbon dioxide reacted with sodium (eq 16) faster than with the oxide ion (eq 8). The consumption of only 35% of the carbon dioxide required by the stoichiometry of eq 17 was apparently due to the very slow rate of consumption after 50 min, and thus the difference between the sparge gas and exhaust gas concentrations was too small to be detected. The fact that the CO_2^{2-} ion was the predominant species in the melt sparged with carbon dioxide suggets that the rate of CO_2^{2-} ion decomposition (eq 9) was slower than the rate of its formation (eq 16). Similarly, with low carbon dioxide concentration (i.e., nitrogen sparge), the CO_2^{2-} ion apparently decomposed as rapidly as it formed, and thus the only wave observed was that due to carbon monoxide.

$$2Na + CO_2 \rightarrow Na_2CO_2 \quad (16)$$

$$Na_2CO_2 \rightleftarrows Na_2O + CO \quad (9)$$

$$Na_2O + CO_2 \rightleftarrows Na_2CO_3 \quad (8)$$

$$2Na + 2CO_2 \rightarrow Na_2CO_3 + CO \quad (17)$$

Graphite Electrode. The cell was modified such that offgases from a graphite working electrode could be isolated and analyzed independent of the bulk exhaust. The melt was sparged with carbon dioxide (10.40%) in nitrogen overnight prior to installation of the graphite electrode. The graphite electrode was installed, allowed to hang from a platinum lead wire 1 cm above the melt until steady state was achieved, and then lowered into the melt such that approximately 2 cm of the electrode was submerged providing a geometric surface area of approximately 2 cm^2. The rest potential was −1.254 V. Potentiostatic measurements were made, and the exhaust gas from the graphite electrode was analyzed. The results (Table II) showed that the oxidation rate of the graphite electrode increased by a factor of 4 when the electrode was lowered into the melt and that application of positive potentials (relative to the rest potential) increased the oxidation rate dramatically. Similarly, application of negative potentials decreased the oxidation rate.

Table II. Graphite Electrode Gasification Rate as a Function of Applied Potential

app pot., V	rel pot., V	steady-state exhaust CO concn, %	current, mA
electrode out of melt		0.02	
−0.500	+0.754	0.99	−75
−0.750	+0.504	0.51	−38
−0.900	+0.354	0.31	−25
−1.254	0	0.08	0
−1.500	−0.246	0.05	+9
−1.600	−0.346	0.00	+25

Table III. Proposed Sequence of Reactions in Air-Sparged Sodium Carbonate Melt[5]

$Na_2CO_3 \rightleftarrows Na_2O + CO_2$	(8)
$Na_2O \rightleftarrows 2Na + {}^1/_2O_2$	(18)
$Na_2CO_3 + {}^1/_2O_2 \rightleftarrows Na_2CO_4$	(19)
$Na_2CO_4 \rightleftarrows Na_2O_2 + CO_2$	(20)
$Na_2CO_4 + CO_2 \rightleftarrows Na_2C_2O_6$	(21)
$Na_2O_2 + O_2 \rightleftarrows 2NaO_2$	(14)
$Na_2O_2 \rightleftarrows Na_2O + {}^1/_2O_2$	(22)

A similar experiment employing a graphite working electrode was attempted in air-sparged melt. The rest potential was −0.92 V. The oxidation of the electrode under the conditions was sufficiently rapid that no change in the rate was observed by application of relative positive or negative potentials. The rest potential of −0.92 V in the air-sparged system compared to −1.254 V in the carbon dioxide sparged system suggests that the metallic sodium produced at the surface of the graphite electrode reacted faster with oxygen or with oxyanions in the melt than with carbon dioxide.

Discussion

On the basis of observed changes in the composition of sodium carbonate melts that resulted from perturbations of the carbon dioxide and oxygen concentrations of the sparge gas and additions of sodium oxide, sodium peroxide, and sodium superoxide, assignments of five of the eight electrochemical waves observed were made (Table I).[5] A sequence of equilibria was proposed that accounts for the interconversion of melt species (Table III).[5]

The results of this work show that the addition of graphite to air-sparged sodium carbonate melt caused the peak currents of electrochemical waves assigned to superoxide, peroxycarbonate, peroxydicarbonate, and oxide ions to decrease and the wave assigned to peroxide ion to increase. A control experiment in which no graphite was present in the melt showed that the decreases in the peak currents of waves due to superoxide, peroxycarbonate, and oxide ions and the increase in the peak current of peroxide ion during graphite oxidation were probably due to the increased carbon dioxide concentration and not directly to the added graphite. Of the electroactive species observed, only the wave assigned to peroxydicarbonate ion exhibited a significant difference between the oxidation and control experiments, which suggests that the peroxydicarbonate ion may react directly with graphite faster than with carbon dioxide.

Graphite added to nitrogen-sparged melt resulted in the production of carbon monoxide, a cathodic shift of the rest potential to −1.370 V, decreases in the peak currents of waves assigned to superoxide, peroxycarbonate, and peroxydi-

carbonate ions, an increase in the peak current of the wave due to the peroxide ion, and the buildup of waves assigned to carbon monoxide and the CO_2^{2-} ion. Under similar conditions, the addition of sodium metal also resulted in the production of carbon monoxide, a cathodic shift of the rest potential to −1.185 V, and a buildup of the wave assigned to carbon monoxide. No CO_2^{2-} ion was observed until carbon dioxide containing gas was sparged. Similarly, graphite added to melt sparged with carbon dioxide/nitrogen mixtures resulted in the nearly stoichiometric consumption of carbon dioxide and production of carbon monoxide (eq 15), a cathodic shift of the rest potential to −0.925 V, and the appearance of the CO_2^{2-} ion in the melt. The addition of sodium to a similar melt resulted in the consumption of carbon dioxide, the production of carbon monoxide, a cathodic shift of the rest potential to −0.934 V, and the appearance of the CO_2^{2-} ion. Thus, addition of graphite or sodium metal to sodium carbonate melt in the absence of oxygen produced similar results. This suggests that an initial step in the oxidation of graphite was the reduction of sodium ion to produce sodium metal.

Several electron-transfer mechanisms have been proposed for the alkali-metal carbonate catalyzed oxidation of carbon.[1] Among these is a proposal that alkali metals form positive ions (e.g., Na^+) at the carbon surface, decrease the potential energy to oxygen adsorption, and cause increased oxidation rates.[12] Another suggests that alkali metal produced by the decomposition of the corresponding carbonate (e.g., eq 8 and 18) intercalates into graphite and acts as an electron donor, thus influencing the adsorption and desorption of oxygenated species.[13] Both of these proposals suggest that electrons are transferred from the alkali metal to carbon at temperatures near the melting point of the corresponding alkali-metal carbonate. This is unlikely in view of the results discussed above in which sodium metal was apparently produced by the addition of graphite to the melt. Indeed, one of the earliest industrial methods for the production of metallic sodium was the reduction of sodium carbonate with carbon at 1100 °C.[14] The subject of "carbothermic reduction of sodium carbonate" has been studied more recently, and the results have been summarized.[15] At lower temperatures (~400 °C), sodium reacts with graphite to form lamellar materials.[16] Part of the sodium consumed becomes chemically inert, and part remains active (e.g., liberates hydrogen from water). At ambient temperature, the alkali metals clearly transfer one electron to polyaromatic compounds (e.g., naphthalene, anthracene, etc.);[17] the complexes are unstable at higher temperatures, and specific ethereal solvents are required to stabilize them even at ambient temperature. Many of the reactions of these complexes resemble those of alkali metals. For example, sodium–naphthalene complex reacts with mercury to produce sodium amalgam and with water to produce hydrogen.[14] All of the reactions of alkali metals with graphite or graphite model compounds (e.g., anthracene) discussed above indicate that electrons are transferred to carbon only at temperatures lower than those typically employed in carbon oxidation. Thus, proposed mechanisms for alkali-metal carbonate catalyzed carbon oxidation that involve transfer of electrons from alkali metal to carbon would appear unlikely.

The reduction of sodium ions by graphite necessarily produces positive centers in the graphite matrix. The positive centers produced are apparently attacked by anions in the melt, and thus the oxidation process proceeds. A sequence of reactions that is consistent with the data presented here and with data reported previously[4,5] is represented by eq 8, 9, 16, 23, and 24 for graphite oxidation with carbon dioxide sparge and

$$Na_2CO_3 + C \rightarrow 2Na + CO_3^{2-} + \text{"}C^{2+}\text{"} \quad (23)$$

$$\text{"}C^{2+}\text{"} + CO_3^{2-} \rightarrow CO + CO_2 \quad (24)$$

$$2Na + CO_2 \rightarrow Na_2CO_2 \quad (16)$$

$$Na_2CO_2 \rightarrow Na_2O + CO \quad (9)$$

$$Na_2O + CO_2 \rightleftarrows Na_2CO_3 \quad (8)$$

$$C + CO_2 \rightleftarrows 2CO \quad (15)$$

eq 23 and 25–28 for oxidation with air sparge. The overall processes are represented by eq 15 and 29, respectively.

$$Na_2CO_3 + C \rightarrow 2Na + CO_3^{2-} + \text{"}C^{2+}\text{"} \quad (23)$$

$$\text{"}C^{2+}\text{"} + Na_2C_2O_6 \rightarrow 3CO_2 + 2Na^+ \quad (25)$$

$$2Na^+ + CO_3^{2-} \rightarrow Na_2CO_3 \quad (26)$$

$$2Na + O_2 \rightarrow Na_2O_2 \quad (27)$$

$$Na_2O_2 + 2CO_2 \rightarrow Na_2C_2O_6 \quad (28)$$

$$C + O_2 \rightarrow CO_2 \quad (29)$$

With nitrogen sparge, the oxidation of graphite appears to proceed through the same initial steps as with carbon dioxide sparge (eq 9, 16, 23, and 24). However, with the low concentration of carbon dioxide in nitrogen-sparged experiments, sodium oxide was apparently reduced preferentially by graphite (eq 30). Thus, the overall process for graphite oxidation in

$$Na_2O + C \rightarrow 2Na + CO \quad (30)$$

sodium carbonate melt under nitrogen sparge may be represented by eq 31, which is just the carbothermic reduction of

$$Na_2CO_3 + 2C \rightarrow 2Na + 3CO \quad (31)$$

sodium carbonate.[15] This overall process has been proposed previously as the initial step in the mechanism of carbon oxidation catalyzed by alkali-metal carbonates.[18,19]

The first step in these sequences of reactions (eq 23) involves the transfer of electrons from carbon to sodium ions in the melt producing sodium metal and positive centers in the carbon matrix designated "C^{2+}" for convenience. In fact, such centers are more likely to be delocalized. The second step in the proposed sequences (eq 24 and 25) involves the attack of anions in the melt on the positive centers thus produced. The rate of the attack is a function of the anions present. Thus, under carbon dioxide sparge or nitrogen sparge where the initial concentrations of all of the anions with the exception of carbonate ion were essentially zero, the rate of oxidation was approximately 6.5 times slower than in the air-sparged experiment where measurable concentrations of oxide, superoxide, peroxycarbonate, and peroxydicarbonate ions existed. Indeed, the data suggest that the peroxydicarbonate ion reacted fastest. The fact that the oxidation rate of a graphite electrode could be increased by application of a relative positive potential and decreased by application of a relative negative potential (Table II) clearly supports such an ionic mechanism. The processes represented by eq 24 and 25 may initially involve the transfer of an oxide ion (O^{2-}) from an anion in the melt to a positive center in the carbon matrix (eq 32), giving rise

(12) Heuchamps, C. Thesis Ingenieur-Docteur, University de Nancy, 1960.
(13) Franke, F. H.; Meraikib, M. *Carbon* **1970**, *8*, 423.
(14) Lemke, C. H. "Encyclopedia of Chemical Technology"; Wiley: New York, 1969; Vol. 18, p 432.
(15) Holzmann, R. T. "Production of the Boranes and Related Research"; Academic Press: New York, 1967; p 11.
(16) Sleppy, W. C. *Inorg. Chem.* **1966**, *5*, 2021.
(17) Scott, N. D.; Walker, J. F.; Hansley, V. L. *J. Am. Chem. Soc.* **1936**, *58*, 2442.
(18) McKee, D. W.; Chatterji, D. *Carbon* **1975**, *13*, 381.
(19) Veraa, M. J.; Bell, A. T. *Fuel* **1978**, *57*, 194.

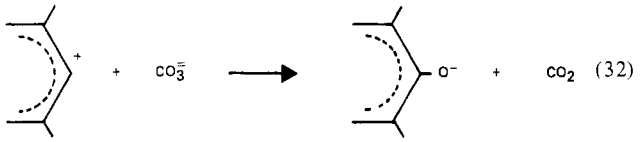

(32)

to a phenoxide-type intermediate. Such intermediates have been shown to exist in potassium carbonate impregnated samples of Spherocarb that had been maintained at 704 °C for 33 min in inert atmosphere.[20] A similar mechanism was reported recently for steam gasification of coal char[21] and probably also operates in the aqueous Fe(III) oxidation of carbon.[22] A number of successive steps are possible to account for the ultimate decomposition of the phenoxide analogue to produce carbon monoxide. An example is the transfer of the negative charge on the bound oxygen atom to another positive center in the carbon matrix, allowing desorption of carbon monoxide from the locally "neutral" carbon matrix.

The proposed sequences of reactions are clearly oversimplified. At least in air-sparged melts, all of the reactions represented in Table III probably participate in the overall oxidation process (e.g., give rise to the overall half-order dependence of the rate on oxygen pressure). Thus, in eq 25, peroxydicarbonate is shown as the active anionic species (as the data suggest); however, the other oxyanions present in air-sparged melts, including carbonate ion, probably also participate. The overall rate of the carbon oxidation process catalyzed by a given alkali-metal carbonate is probably primarily governed by the concentrations of the anions present. However, the fact that the overall rate is dependent on the graphite surface area throughout the process and that the dependence approaches first order as the graphite is nearly consumed indicates that the initial step (eq 23) is also important, and clearly this step is important in determining the overall rates of oxidation processes in which different alkali-metal carbonate catalysts are compared (e.g., sodium vs. potassium).

Acknowledgment. The Department of Energy, Office of Basic Energy Sciences, is gratefully acknowledged for supporting this work under Contract DE-AT03-76ER70030.

Registry No. Na_2CO_3, 497-19-8; O_2^-, 11062-77-4; O_2^{2-}, 14915-07-2; CO_4^{2-}, 34099-49-5; $C_2O_6^{2-}$, 34099-48-4; CO_2, 124-38-9; CO_2^{2-}, 12709-62-5; CO, 630-08-0; N_2, 7727-37-9; Na, 7440-23-5; graphite, 7782-42-5.

(20) Mims, C. A.; Pabst, J. K. *Fuel* **1983**, *62*, 176.
(21) Wood, B. J., et al. Proceedings—International Conference on Coal Science, Pittsburgh, PA, Aug 15-19, 1983.
(22) Dhooge, P. M.; Park, S.-M. *J. Electrochem. Soc.* **1983**, *130*, 1539.

Contribution No. 6846 from the Arthur Amos Noyes Laboratories, Division of Chemistry and Chemical Engineering, California Institute of Technology, Pasadena, California 91125

Electron Exchange between $Cu(phen)_2^+$ Adsorbed on Graphite and $Cu(phen)_2^{2+}$ in Solution

CHI-WOO LEE and FRED C. ANSON*

Received May 19, 1983

The bis(1,10-phenanthroline) complexes of Cu(I) and Cu(II) are both adsorbed on pyrolytic graphite electrodes from aqueous chloride electrolytes. The adsorption of the Cu(II) complex reaches a full monolayer at a concentration of ca. 0.1 mM. The Cu(I) complex appears to oligomerize both in solution and in the adsorbed layer. As a result, much larger quantities of the Cu(I) complex can be deposited on the electrode surface. Rotating-disk voltammetric measurements of the reduction of $Cu(phen)_2^{2+}$ at electrodes coated with a deposit of the Cu(I) complex were utilized to measure the rate of electron transfer between the two complexes. This rate was independent of the quantity of Cu(I) deposited on the electrode, indicating that only the outermost layer of relatively impervious deposit participated in the electron exchange. An estimate of ca. 10^5 M^{-1} s^{-1} was obtained for the rate constant governing the self-exchange reaction.

One of the simplest methods for attaching metal complexes to the surfaces of graphite electrodes takes advantage of the high affinity for graphite of molecules having multiple aromatic centers.[1] Coordination of polypyridine ligands to metal centers creates complexes that show affinity for graphite surfaces, and we have exploited this fact to bind the bis(1,10-phenanthroline) (1,10-phenanthroline = phen) complexes of Cu(II) and Cu(I) to pyrolytic graphite electrodes from aqueous media. In addition, the Cu(I) complex appears to oligomerize in solution. This enhances its tendency to accumulate at the graphite solution interface and causes large quantities of the complex to deposit on the electrode surface. The rate of electron transfer between the deposited $Cu(phen)_2^+$ complex and $Cu(phen)_2^{2+}$ ions dissolved in solution was measured by means of rotating-disk electrode voltammetry.[2,3] This electron-transfer rate is of interest in assessing the potential of deposited $Cu(phen)_2^+$ as an electrocatalyst for the reduction of dioxygen.[4] In addition, there is disagreement in the literature regarding the rate of homogeneous electron exchange between $Cu(phen)_2^+$ and $Cu(phen)_2^{2+}$,[5] and we expected that an electrochemical estimate of the same rate could help to resolve the disagreement.

Experimental Section

Materials. $Cu(phen)_2Cl_2 \cdot 3H_2O$ was prepared by dissolving a slight excess of 1,10-phenanthroline hydrate (J. T. Baker Co.) in warm ethanol and adding it to a solution of $CuCl_2 \cdot 2H_2O$ dissolved in an equal volume of warm water. The crystals that formed after the solution stood overnight were collected, washed with ethanol, and dried under vacuum. Anal. Calcd: C, 52.51; H, 4.04; Cl, 12.92. Found: C, 53.30; H, 4.03; Cl, 13.03.

All other chemicals were reagent grade and were used as received. Solutions were prepared from laboratory deionized water that was passed through a purification train (Barnsted Nanopure) before use. Solutions were deoxygenated with prepurified argon and buffered at

(1) (a) Brown, A. P.; Koval, C.; Anson, F. C. *J. Electroanal. Chem. Interfacial Electrochem.* **1976**, *72*, 379. (b) Brown, A. P.; Anson, F. C. *Ibid.* **1977**, *83*, 203.
(2) Levich, V. G. "Physicochemical Hydrodynamics"; Prentice-Hall: Englewood Cliffs, NJ, 1962; Chapter VI.
(3) Oyama, N.; Anson, F. C. *Anal. Chem.* **1980**, *52*, 1192. Shigehara, K.; Oyama, N.; Anson, F. C. *Inorg. Chem.* **1980**, *20*, 518.
(4) Shigehara, K.; Anson, F. C. *J. Electroanal. Chem. Interfacial Electrochem.* **1982**, *132*, 107.
(5) (a) Yoneda, G. S.; Blackmer, G. L.; Holwerda, R. A. *Inorg. Chem.* **1977**, *16*, 3776. (b) Augustin, M. A.; Yandell, J. K. *Ibid.* **1979**, *18*, 577.
(6) Oyama, N.; Anson, F. C. *J. Am. Chem. Soc.* **1979**, *101*, 3450.

0020-1669/84/1323-0837$01.50/0